Structural and magnetotransport properties of the colossal magnetoresistance material $Tl_2Mn_2O_7$

Y. Shimakawa, Y. Kubo, T. Manako, and Y. V. Sushko
Fundamental Research Laboratories, NEC Corporation, 34 Miyukigaoka, Tsukuba 305, Japan

D. N. Argyriou and J. D. Jorgensen
Materials Science Division, Argonne National Laboratory, Argonne, Illinois 60439
(Received 18 July 1996)

The crystal structure and its variation with temperature of the spin-charge coupled material $Tl_2Mn_2O_7$ pyrochlore is investigated. Structure refinement from the neutron powder-diffraction data reveals that $Tl_2Mn_2O_7$ has nearly stoichiometric composition and is crystallized in the cubic-pyrochlore-type structure with a characteristic Mn-O-Mn bond angle of 133°. There is no structural anomaly associated with the change in magnetotransport properties at 142 K, suggesting weak spin-lattice and charge-lattice correlations. Despite the similarity of magnetotransport properties observed in the perovskite and the pyrochlore colossal magnetoresistance manganese oxides, the double-exchange mechanism, which is usually applied to the perovskite materials, does not seem to explain the behavior in the pyrochlore $Tl_2Mn_2O_7$ compound. A superexchange-type interaction may stabilize the ferromagnetic ordering of Mn spins and cause the metallic conduction at low temperatures in $Tl_2Mn_2O_7$. [S0163-1829(97)00910-7]

I. INTRODUCTION

Hole-doped perovskite manganese oxides, e.g., $La_{1-x}Sr_xMnO_3$, have attracted considerable attention because they exhibit intrinsic colossal magnetoresistance (CMR).[1–4] A number of studies on these materials have revealed that spin, charge, and lattice in this system are strongly correlated. Hole doping into the antiferromagnetic insulating compound $LaMnO_3$ with Mn^{3+} produces Mn^{4+} ions, and thus creates itinerant e_g holes. A double-exchange interaction between Mn^{3+} and Mn^{4+} mediates ferromagnetic ordering and the compound shows metallic conduction below the ferromagnetic Curie temperature (T_C).[5–7] Electron transfer depends on local spin alignment. Therefore, there is a strong correlation between spin and charge, giving rise to the CMR observed at temperatures near T_C. In addition, lattice anomalies associated with changes in spin alignment and/or electron transfer are often observed, suggesting a correlation between spin and lattice. In at least one system, a change in the crystal structure can be induced by applying a magnetic field.[8] Static and/or dynamic Jahn-Teller distortions of the MnO_6 octahedra are also suspected to play an important role in the behavior.[9] Surprisingly large changes in structural parameters such as lattice constants, bond lengths, and thermal parameters are observed at the ferromagnetic and/or metal-insulator transition temperatures.[10–12] Such spin-charge-lattice coupled phenomena shed light on an area of solid-state physics and also suggest potential technological applications.

Another spin-charge coupled material was recently discovered: The compound is $Tl_2Mn_2O_7$ with the pyrochlore structure.[13] $Tl_2Mn_2O_7$ shows ferromagnetic behavior below 142 K and undergoes a sharp drop in resistivity around this temperature. The resistivity decrease with the development of spontaneous magnetization and the colossal magnetoresistive change with an applied magnetic field suggest a strong correlation between spin and charge in this system. Although the observed magnetotransport properties of $Tl_2Mn_2O_7$ are quite similar to those observed in perovskite manganese oxides, the pyrochlore $Tl_2Mn_2O_7$ compound differs both structurally and electronically from the perovskites. Both the perovskite and pyrochlore manganese oxides consist of MnO_6 octahedra with shared vertexes. The structural networks, however, are completely different. The pyrochlore structure has a three-dimensional array with a large bend of the Mn-O-Mn bond angle (Fig. 1). In $Tl_2Mn_2O_7$ the metallic conduction results from a small electron doping (0.001–0.005 per formula unit) into Mn^{4+} with a $(3d)^3$ configuration. This is in sharp contrast to the $La_{1-x}Sr_xMnO_3$ perovskite, where a fairly large number of holes (about 0.18 per formula unit) are introduced into Mn^{3+} with a $(3d)^4$ configuration. Because the magnetotransport properties, including CMR, are quite similar in the perovskite and pyrochlore manganese oxides, one might expect the same mechanism based on the double-exchange theory for the magnetotransport behaviors in the two compounds. However, considering the significant differences in the crystal structure and the electronic structure of the two compounds, an ambiguity remains as to whether the double-exchange interaction is the only mechanism for stabilizing the ferromagnetic and metallic state at low temperatures in $Tl_2Mn_2O_7$.

This paper describes the crystal structure of $Tl_2Mn_2O_7$ and the structural changes over the temperature range from 300 to 20 K determined from x-ray and neutron-diffraction data. Magnetotransport properties of the compound are also reported. We see similarities and differences between the perovskite and pyrochlore materials, and discuss the mechanism for stabilizing the ferromagnetic and metallic state of the $Tl_2Mn_2O_7$ compounds. Data for the pyrochlore $In_2Mn_2O_7$, which is isostructural to $Tl_2Mn_2O_7$, are also reported. Magnetic and transport properties of this material are compared with those of $Tl_2Mn_2O_7$.

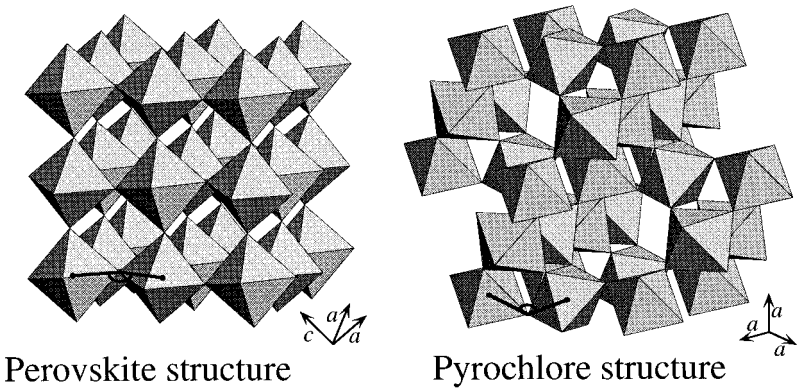

FIG. 1. Networks of the MnO_6 octahedra in the perovskite and pyrochlore structures. The perovskite structure shown has rhombohedral symmetry as is seen in $La_{0.825}Sr_{0.175}MnO_3$. Rhombohedral axes for the perovskite structure and cubic axes for the pyrochlore structure are shown with arrows. Mn ions are located in the center of the octahedra. La and Sr atoms in the $La_{0.825}Sr_{0.175}MnO_3$ perovskite and Tl and O(2) atoms in the $Tl_2Mn_2O_7$ pyrochlore are not displayed.

II. EXPERIMENTS

Powder samples of $Tl_2Mn_2O_7$ and $In_2Mn_2O_7$ were synthesized by solid-state reaction under high pressure conditions. A mixture of Tl_2O_3 or In_2O_3 and MnO_2 was sealed in a gold capsule and allowed to react in a high pressure apparatus at 2.5 GPa at 1000–1150 °C for 30 min. After grinding, the sample was sintered again under the same conditions to achieve high quality and high density. The sample was rapidly cooled to room temperature before releasing the pressure. The applied pressure of 2.5 GPa is lower than the 5–6 GPa synthesis pressures reported in the literature,[14,15] but it seems to be enough for the formation of the pyrochlore $Tl_2Mn_2O_7$. 200–500 mg samples were obtained by this procedure.

X-ray powder-diffraction data were taken by a conventional θ–2θ scanning method. Time-of-flight neutron powder-diffraction data were collected with a closed-cycle helium refrigerator on the Special Environment Powder Diffractometer at Argonne's Intense Pulsed Neutron Source. The crystal structures were refined by the Rietveld technique using the programs RIETAN (Ref. 16) and GSAS (Ref. 17).

Magnetic and transport properties were investigated in the temperature range from 5 to 350 K by measuring dc magnetization using a superconducting quantum interference device magnetometer and four-probe resistivity, respectively.

III. RESULTS AND DISCUSSION

The $Tl_2Mn_2O_7$ sample was confirmed to be almost single phase by both x-ray and neutron powder-diffraction data. Figure 2 shows examples of x-ray and neutron-diffraction patterns and their Rietveld refinement profiles. Sharp Bragg peaks observed in the diffraction patterns show that the $Tl_2Mn_2O_7$ sample is well crystallized in the face-centered-cubic pyrochlore-type structure with a space group of $Fd3m$.

Table I lists the results of structural refinement for $Tl_2Mn_2O_7$ from the neutron-diffraction data obtained at room temperature. The refined occupancies indicate a nearly stoichiometric composition of $Tl_2Mn_2O_7$. If we assume ionic valences of $+3$ for Tl and -2 for O ions, the stoichiometric composition of $Tl_2Mn_2O_7$ gives a valence state of $+4$ for Mn ion from a simple ionic consideration. This is consistent with other observations such as the value of the saturated magnetic moment at low temperature and the small number of conduction electrons observed by Hall coefficient measurements.[13,15] In the ionic model, the Mn^{4+} state in $Tl_2Mn_2O_7$ indicates no apparent chemical doping in the system.

The bond distance and angle between Mn and O in the MnO_6 octahedra for $Tl_2Mn_2O_7$ are listed in Table II. The Mn^{4+} ion has a $(t_{2g})^3$ electron configuration, and thus the $Mn^{4+}O^{2-}{}_6$ octahedron shows no Jahn-Teller distortion. The six Mn-O bonds in the octahedron are identical. The ob-

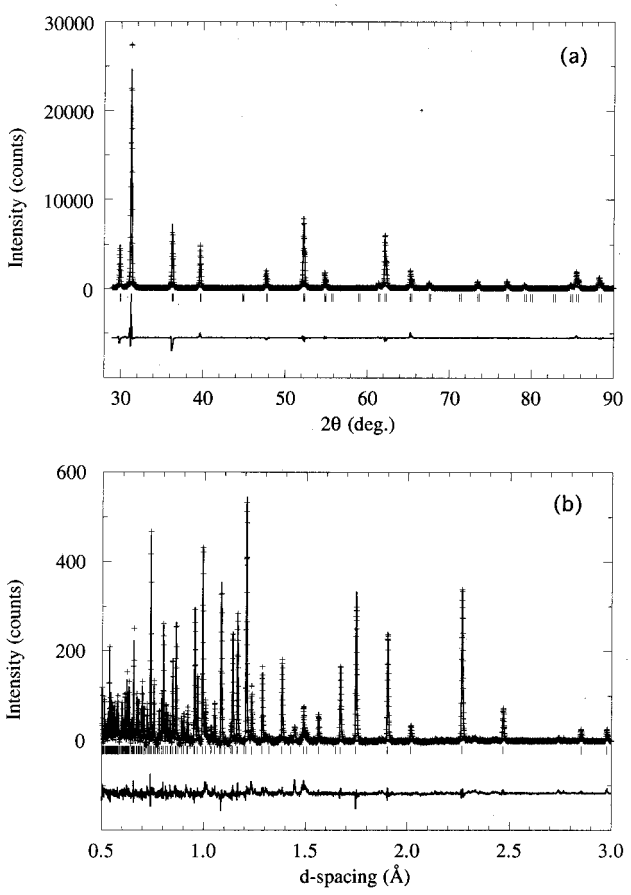

FIG. 2. (a) Room-temperature x-ray and (b) 20-K neutron-diffraction patterns for $Tl_2Mn_2O_7$ and the Rietveld refinement profiles. The raw diffraction data are shown as plus marks; the calculated profile is shown as a solid line. Tick marks below the profile mark the positions of allowed reflections. The differences between the observed and the calculated intensities are shown at the bottom. Analysis of the 20-K neutron-diffraction data includes magnetic scattering (see text).

TABLE I. Refined structural parameters for $Tl_2Mn_2O_7$. B_{iso} is the isotropic thermal parameter and n is the occupancy. Numbers in parentheses are standard deviations of the last significant digit. $R(wp)=10.81\%$, $R(p)=6.68\%$, $R(F^2)=9.26\%$.

Space group, $Fd\bar{3}m$		$a=9.89093$ (7) Å				
Atom	Position	x	y	z	B_{iso} (Å^2)	n
Tl	16d	0.5	0.5	0.5	0.58(4)	0.97(2)
Mn	16c	0.0	0.0	0.0	0.38(6)	1.0
O(1)	48f	0.3261(1)	0.125	0.125	0.67(4)	1.00(2)
O(2)	8b	0.375	0.375	0.375	0.78(6)	1.07(2)

served bond distance of 1.90 Å is typical for a Mn^{4+} ion coordinated to six oxygen atoms, but is significantly smaller than those observed in the perovskite manganese oxides. In $La_{0.7}Sr_{0.3}MnO_3$ with an average ionic state of Mn of +3.3, a Mn-O bond length of about 1.96 Å is observed.[18] Another distinguishing feature of the crystal structure is the Mn-O-Mn bond angle of about 133°. This bond angle is quite small compared with those in the perovskite CMR compounds, where bond angles of 155–170° are typically observed (see Fig. 1).[18] Although both pyrochlore and perovskite manganese oxides are conducting ferromagnets, such significant differences in the bond distances and angles should cause some differences in electron transfer and magnetic interaction in these materials. This point is discussed later.

Within the precision of the measurement, there is no structural anomaly associated with the change in magnetotransport properties for $Tl_2Mn_2O_7$ in the temperature range from 300 to 20 K. As shown in Fig. 3, no anomalies in the temperature dependence of lattice parameter, Mn-O bond length, and Mn-O-Mn bond angle are observed. The lattice parameter decreases smoothly with decreasing temperature. The Mn-O bond length is nearly constant, while the Mn-O-Mn bond angle changes about 0.25% over the measured temperature range. Thus, in the $Tl_2Mn_2O_7$ pyrochlore the MnO_6 octahedron is essentially rigid, but the tilting angle of the octahedron (connecting angle to neighboring octahedra) changes with decreasing temperature. Such behavior is in sharp contrast to experimental results for the perovskite compounds, which show a strong correlation between spin and lattice. Abrupt changes in lattice parameters, corresponding to a volume change of $\Delta V/V=0.13\%$, are observed at the ferromagnetic and metal-insulator transition temperature for the $La_{0.8}Ca_{0.2}MnO_3$ compound.[11] Substantial changes in two equatorial Mn-O bond lengths (2.7%) at T_C are also reported in the insulating $La_{0.875}Sr_{0.125}MnO_3$ material, indicating a change in the magnitude of the Jahn-Teller distortion of the MnO_6 octahedron.[12]

Ferromagnetic ordering of the Mn spins at low temperatures is observed by both dc magnetization and additional scattering in the neutron-diffraction data. Figure 4 shows the temperature dependence of the magnetization for $Tl_2Mn_2O_7$ measured at an applied magnetic field of 0.5 T. In the inset of the Fig. 4, the magnetic-field dependence of the magnetization at 5 K is also shown. Ferromagnetic behavior is observed below 142 K. The saturated magnetization at low temperature is $3.0\mu_B$, which is the expected value for ferromagnetic ordering of Mn^{4+} ions with a $(3d)^3$ configuration ($S=3/2$), though a saturated moment of only $2.59\mu_B$ was

TABLE II. The Mn-O bond distance and the Mn-O-Mn bond angle for $Tl_2Mn_2O_7$. Numbers in parentheses are standard deviations of the last significant digit.

Mn-O(1) (Å)	1.9034(6)
Mn-O(1)-Mn (°)	133.44(8)

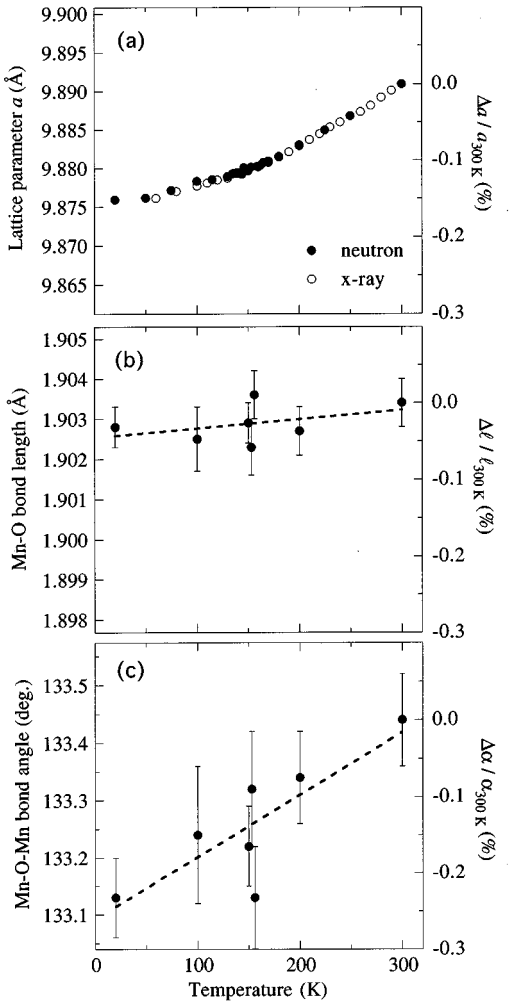

FIG. 3. Temperature dependence of (a) lattice parameter, (b) Mn-O bond length, and (c) Mn-O-Mn bond angle for $Tl_2Mn_2O_7$. Data plotted as closed symbols are obtained by Rietveld analyses from neutron-diffraction data. Open symbols are from x-ray diffraction data. Dotted lines for the changes in the Mn-O bond length and the Mn-O-Mn bond angle are a guide to the eye.

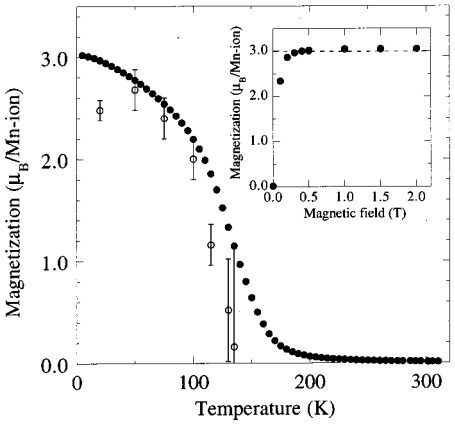

FIG. 4. Temperature dependence of the magnetization for $Tl_2Mn_2O_7$ measured at an applied magnetic field of 0.5 T (closed symbols). The inset shows the magnetic-field dependence of the magnetization at 5 K. Refined magnetic moments from the Rietveld analyses of the neutron-diffraction data are also shown in the figure with open symbols.

observed for the previous sample in Ref. 13 due to the presence of impurity phases. The neutron-diffraction pattern at 20 K shows additional intensity which originates from magnetic scattering. In the Rietveld analysis, models including the magnetic scattering significantly improve the refinements. Results of the refinements based on four models are listed in Table III. Model 1 considers only nuclear scattering from constituent atoms. In models 2, 3, and 4, both nuclear scattering and magnetic scattering from ferromagnetically ordered spins at Mn site along [1 0 0], [1 1 1], and [−2 1 1] directions, respectively, are considered. The refinements based on models 2, 3, and 4 give lower values for the goodness of fit (GOF) than model 1, suggesting the ferromagnetic long-range ordering of Mn spins. Refined magnetic moments of 2.4–2.5μ_B are in reasonable agreement with the observed saturated dc moments. Although the neutron-diffraction data at low temperatures support the ferromagnetic component of the long-range ordering of Mn spins, our analysis does not give a unique solution for the magnetic structure for $Tl_2Mn_2O_7$. Considering that the pyrochlore structure represents a geometrically highly frustrated system in the presence of antiferromagnetic interaction,[19,20] the actual magnetic structure may be rather complicated (e.g., slightly canted, spiral, etc.). The smaller values of the refined magnetic moment from the neutron-diffraction data (2.4–2.5μ_B) than the observed dc moment (3.0μ_B) may indicate such a complicated magnetic structure. The additional intensity from the magnetic scattering decreases with increasing temperature, and vanishes above 140 K. The neutron-diffraction pattern at 20 K with the refined profile based on model 2 is shown in Fig. 2(b). The temperature dependence of the refined magnetic moment from the neutron-diffraction data (also shown in Fig. 4) agrees with that of the dc moment measurements.

TABLE III. Agreement indices of Rietveld analysis of neutron-diffraction data for $Tl_2Mn_2O_7$ obtained at 20 K based on the following four models. Goodness of fit (GOF) is defined as sum of the squares of the deviations χ^2. M is the refined magnetic moment. Model 1, Scattering from only nuclears (N) is considered. Model 2, Scattering from nuclears and ferromagnetically ordered spins (M) along the [1 0 0] direction are considered. Model 3, Same as for model 2, but with spins along the [1 1 1] direction. Model 4, Same as for model 2, but with spins along the [−2 1 1] direction.

Models	$R(wp)$	$R(p)$	GOF (χ^2)	M (μ_B)
1:N	11.34	7.14	2.24	
2:$N+M$[1 0 0]	11.22	7.05	2.17	2.5(1)
3:$N+M$[1 1 1]	11.23	7.06	2.18	2.4(1)
4:$N+M$[−2 1 1]	11.22	7.05	2.18	2.4(1)

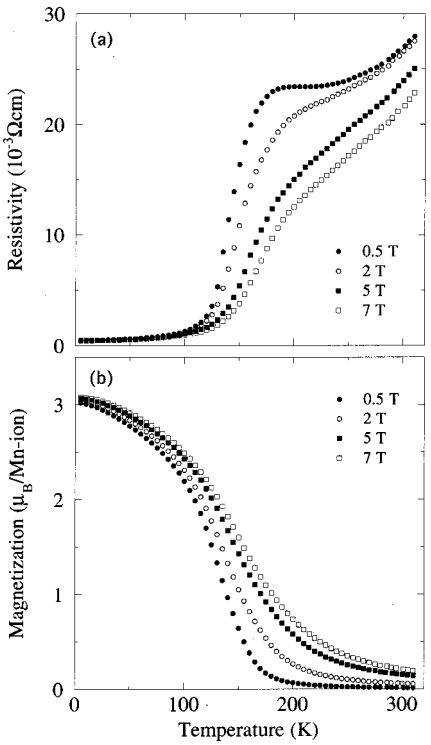

FIG. 5. Temperature dependence of (a) the resistivity and (b) the magnetization for $Tl_2Mn_2O_7$ measured at applied magnetic fields of 0.5, 2, 5, and 7 T.

Transport properties in $Tl_2Mn_2O_7$ are strongly correlated to the magnetic properties. Figure 5 shows the temperature dependence of the resistivity and the magnetization measured at applied magnetic fields of 0.5, 2, 5, and 7 T. The resistivity decreases are pronounced at magnetic ordering temperatures for all fields. Near the ferromagnetic transition temperature, a large change in resistivity, so-called negative colossal magnetoresistance, is observed with increasing an applied magnetic field. Using the data in Fig. 5, the changes in resistivity are plotted against the changes in magnetization in Fig. 6. The resistivity changes measured under different magnetic fields show an identical behavior to the magnetization. Therefore, the electron transfer in $Tl_2Mn_2O_7$ is closely related to the local spin alignment. Both the sharp drop in resistivity at T_C and the magnetoresistive change near T_C should be governed mainly by magnetic scattering.

The observed magnetotransport properties, including CMR, in the $Tl_2Mn_2O_7$ pyrochlore are quite similar to those

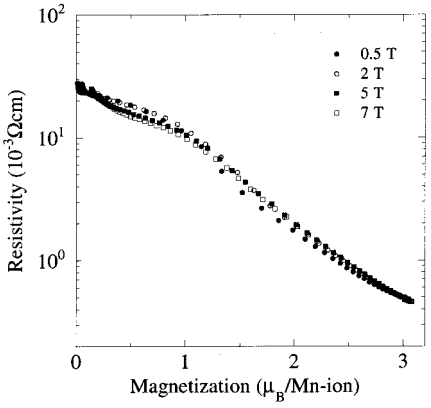

FIG. 6. The change in resistivity plotted against the change in magnetization for $Tl_2Mn_2O_7$ using the data in Fig. 5.

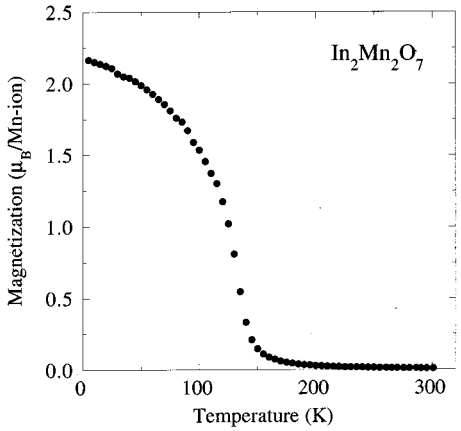

FIG. 7. Temperature dependence of the magnetization for $In_2Mn_2O_7$ measured at an applied magnetic field of 0.5 T.

observed in the perovskite manganese oxides. In the perovskite manganese oxides the magnetotransport properties have been explained within the framework of a double-exchange mechanism.[5–7] In this mechanism, kinetic energy gain by a sufficient number of holes stabilizes the ferromagnetic alignment of the Hund's-rule-coupled Mn spins at low temperatures. A recent theoretical approach on the perovskite CMR materials also points out the importance of lattice effects (electron-phonon interaction) to achieve the observed large change in resistivity.[9] In the context of these scenarios for the CMR mechanism, we see some differences between $Tl_2Mn_2O_7$ and the perovskite compounds. The most distinct difference in the pyrochlore $Tl_2Mn_2O_7$ is the small number of conduction carriers. The observed carrier concentration of 0.001–0.005 electrons per formula unit seems to be too small for stabilizing the ferromagnetic alignment of local spins. Additionally, there is no structural anomaly associated with the change in magnetotransport properties indicating that the spin-lattice and the charge-lattice correlations are weak in the $Tl_2Mn_2O_7$ pyrochlore. The weak charge-lattice coupling might be explained by the small number of carriers. Although our structural analysis does not provide direct information on dynamical and short-range correlations, the observed small thermal parameters for all sites strongly suggest that such effects play a minor role in this system.

A recent study of the effect of pressure on this pyrochlore material also reveals behavior that is not consistent with the double-exchange theory.[21] A reduced Mn-O bond length is expected to increase electron transfer from Mn to Mn *via* oxygen atoms, thus the ferromagnetic transition temperature should increase under pressure. In the perovskite double-exchange ferromagnet, such a positive pressure effect is observed.[22] In contrast, a negative pressure effect on the ferromagnetic Curie temperature has been observed in the pyrochlore $Tl_2Mn_2O_7$ material.

In addition, $In_2Mn_2O_7$, which is isostructural to $Tl_2Mn_2O_7$, shows an interesting contrast with the $Tl_2Mn_2O_7$ compound. As shown in Fig. 7, $In_2Mn_2O_7$ also shows ferromagnetism below about 150 K. Although the saturated magnetic moment at 5 K is $2.17\mu_B$ (72% of the expected value) due to the presence of impurity phases, the essential magnetic behavior is quite similar to that observed in $Tl_2Mn_2O_7$. This material, however, is an insulator both above and below the ferromagnetic transition temperature. In $In_2Mn_2O_7$, therefore, electrical conduction seems to have no relation to the magnetism. The ferromagnetic state at low temperatures is stabilized without being mediated by a kinetic energy gain by conduction carriers.

All these features observed in the pyrochlore materials raise doubts that the behavior can be explained by the same CMR mechanism applied to the perovskite materials, despite the similar magnetotransport properties. Of particular concern is a mechanism for stabilizing the ferromagnetic and metallic state at low temperatures in $Tl_2Mn_2O_7$. As has been discussed by Goodenough, the superexchange interaction in Mn^{4+}-O^{2-}-Mn^{4+} strongly depends on the Mn-O-Mn bond angle.[23] Antiferromagnetic superexchange interaction is expected for 180° cation-anion-cation interaction with d^3 outer electron configurations. Ferromagnetic interaction, in contrast, is often observed for a 90° arrangement. Crossover from the antiferromagnetic to ferromagnetic interaction in the d^3-d^3 cation-anion-cation coupling could occur in the range $125°<\alpha<150°$. The observed Mn-O-Mn bond angle of 133° in $Tl_2Mn_2O_7$ is in the crossover range. If the ferromagnetic superexchange interaction is dominant in the $Tl_2Mn_2O_7$ pyrochlore, the ferromagnetic alignment of Mn spins at low temperatures can be stabilized without mediation by the double-exchange-type electron transfer. This type of superexchange interaction is believed to be responsible for the ferromagnetism in the insulating (semiconducting) pyrochlores $R_2Mn_2O_7$ (R, rare-earth cations), though the T_C values of these compounds are relatively low (20–40 K).[24] In this case, the resistivity change in $Tl_2Mn_2O_7$ results from the effect of the local spin alignment. However, considering that the spin-dependent electron scattering in ordinary metals and alloys gives only a few percent change in resistivity, it remains puzzling why the resistivity in $Tl_2Mn_2O_7$ changes by such a large amount with local spin alignment.

The ferromagnetic and metallic state at low temperatures and the magnetoresistance have some similarities to the s-f interaction seen in europium chalcogenides, EuX (X=O, S, Se, or Te).[25] EuO, for example, shows a ferromagnetic and metallic state below about 70 K. Near the ferromagnetic transition temperature, a similar large magnetoresistance is observed.[26] It is believed that Eu($5d$) and ($5s$) bands mainly contribute to the conduction and a localized Eu($4f$) band is associated with the magnetism. With a strong exchange in-

teraction between the conduction electrons and the localized Eu($4f$) electrons (of the order of 0.1 eV), mobility of the carriers should be affected by the magnetic ordering of the Eu($4f$) spins. Two possible electronic structures for $Tl_2Mn_2O_7$, where a small number of conduction electrons are doped into the e_g or down-spin band of the t_{2g} state depending on the energy difference between Δ_{ex} (exchange interaction of Mn ions) and $10Dq$ (orbital splitting by the crystal field) were discussed in a previous paper.[13] Recent local-density approximation (LDA) band calculations also suggest that contributions from the Tl($6s$) band may play a crucial role in conduction even in the stoichiometric composition.[27] Since the energy level of the Tl($6s$) band is close to the levels of the Mn($3d$) and O($2p$) bands, the Tl($6s$) band can be hybridized with the Mn($3d$) and O($2p$) bands and cross the Fermi level of $Tl_2Mn_2O_7$. In this case, some portion of the electrical conduction originates from the Tl($6s$) band, and the Tl($6s$) electrons are also scattered by the localized Mn($3d$) spins. Thus, the spin-charge coupling in $Tl_2Mn_2O_7$ may be explained by the strong exchange interaction between the Tl($6s$) and Mn($3d$) electrons, which is similar to the s-f interaction seen in europium chalcogenides.

In conclusion, the structural study on a discovered spin-charge coupled $Tl_2Mn_2O_7$ pyrochlore suggests that the spin-lattice and charge-lattice correlations are weak in this material, which is in sharp contrast to the case of perovskite CMR materials. In $Tl_2Mn_2O_7$, superexchange-type interaction, not the double-exchange mechanism, may stabilize the ferromagnetic ordering of Mn spins and cause the metallic conduction at low temperatures in $Tl_2Mn_2O_7$. The discovery of this class of CMR material provides significant insight into the spin-charge coupled physics and could also lead to the discovery of new magnetic and magnetoresistive materials that could be useful for technological applications.

Note added in proof. A recent paper by Subramanian *et al.*[28] described the results of structural refinement of $Tl_2Mn_2O_7$ at room temperature from powder neutron and single-crystal x-ray-diffraction data. They also confirmed the stoichiometric composition of this material and reached the similar conclusion to ours on the CMR mechanism of the $Tl_2Mn_2O_7$ pyrochlore compound.

ACKNOWLEDGMENTS

We thank N. Hamada for helpful discussion and an LDA calculation for $Tl_2Mn_2O_7$. Thanks are also due to M. Mizuta for his support during this work. This work was supported by the NSF Office of Science of Technology Centers under Contract No. DMR 91-20000 (D.N.A.), and the U.S. Department of Energy, Basic Energy Science–Materials Sciences, under Contract No. W-31-109-ENG-38 (J.D.J.).

[1] K. Chahara, T. Ohno, M. Kasai, Y. Kanke, and Y. Kozono, Appl. Phys. Lett. **62**, 780 (1993).
[2] R. von Helmolt, J. Wecker, B. Holzapfel, L. Schultz, and K. Samwer, Phys. Rev. Lett. **71**, 2331 (1993).
[3] S. Jin, T. H. Tiefel, M. McCormack, R. A. Fastnacht, R. Ramesh, and L. H. Chen, Science **264**, 413 (1994).
[4] Y. Tokura, A. Urushibara, Y. Moritomo, T. Arima, A. Asamitsu, G. Kido, and N. Furukawa, J. Phys. Soc. Jpn. **63**, 3931 (1994).
[5] G. H. Jonker and J. H. van Santen, Physica **16**, 337 (1950).
[6] C. Zener, Phys. Rev. **82**, 403 (1951).
[7] P.-G. de Gennes, Phys. Rev. **118**, 141 (1960).
[8] A. Asamitsu, Y. Moritomo, Y. Tomioka, T. Arima, and Y. Tokura, Nature (London) **373**, 407 (1995).
[9] A. J. Millis, P. B. Littlewood, and B. I. Shraiman, Phys. Rev. Lett. **74**, 5144 (1995).
[10] M. R. Ibarra, P. A. Algarabel, C. Marquina, J. Blasco, and J. Garcia, Phys. Rev. Lett. **75**, 3541 (1995).
[11] P. G. Radaelli, D. E. Cox, M. Marezio, S.-W. Cheong, P. E. Schiffer, and A. P. Ramirez, Phys. Rev. Lett. **75**, 4488 (1995).
[12] D. N. Argyriou, J. F. Mitchell, C. D. Potter, D. G. Hinks, J. D. Jorgensen, and S. D. Bader, Phys. Rev. Lett. **76**, 3826 (1996).
[13] Y. Shimakawa, Y. Kubo, and T. Manako, Nature (London) **379**, 53 (1996).
[14] H. Fujinaka, N. Kinomura, M. Koizumi, Y. Miyamoto, and S. Kume, Mater. Res. Bull. **14**, 1133 (1979).
[15] N. P. Raju, J. E. Greedan, and M. A. Subramanian, Phys. Rev. B **49**, 1086 (1994).
[16] F. Izumi, *The Rietveld Method*, edited by R. A. Young (Oxford University Press, Oxford, 1993).
[17] A. C. Larson and R. B. von Dreele, *General Structure Analysis System* (University of California, 1985-1990).
[18] H. Y. Hwang, S.-W. Cheong, P. G. Radaelli, M. Marezio, and B. Batlogg, Phys. Rev. Lett. **75**, 914 (1995).
[19] J. N. Reimers, J. E. Greedan, R. K. Kremer, E. Gmelin, and M. A. Subramanian, Phys. Rev. B **43**, 3387 (1991).
[20] B. D. Gaulin, J. N. Reimers, T. E. Mason, J. E. Greedan, and Z. Tun, Phys. Rev. Lett. **69**, 3244 (1992).
[21] Y. V. Sushko, Y. Kubo, Y. Shimakawa, and T. Manako, Czech. J. Phys. **46**, 2003 (1996).
[22] Y. Moritomo, A. Asamitsu, and Y. Tokura, Phys. Rev. B **51**, 16 491 (1995).
[23] J. B. Goodenough, *Magnetism and the Chemical Bond* (Interscience, New York, 1963).
[24] M. A. Subramanian, C. C. Torardi, D. C. Johnson, J. Pannetier, and A. W. Sleight, J. Solid State Chem. **72**, 24 (1988).
[25] N. Tsuda, K. Nasu, A. Yanase, and K. Siratori, *Electronic Conduction in Oxides* (Springer-Verlag, Berlin, 1991).
[26] M. R. Oliver, J. O. Dimmock, A. L. McWhorter, and T. B. Reed, Phys. Rev. B **5**, 1078 (1972).
[27] N. Hamada *et al.* (unpublished).
[28] M. A. Subramanian, B. H. Toby, A. P. Ramirez, W. J. Marshall, A. W. Sleight, and G. H. Kewi, Science **273**, 81 (1996).